Published in Soft Matter 7, issue 10, 4948-4953, 2011
which should be used for any reference to this work

A liquid-crystalline fullerene–oligophenylenevinylene dyad which displays columnar mesomorphism†

Thi Nhu Y Hoang,[a] Damian Pociecha,*[b] Miroslaw Salamonczyk,[b] Ewa Gorecka[b] and Robert Deschenaux*[a]

The design, synthesis and liquid-crystalline properties of a family of hybrid compounds which are built from rod-like (oligophenylenevinylene) and disc-like [poly(benzyl ether)] units are reported. All compounds form columnar phases within broad temperature ranges; the mesophases are stable even below room temperature. Weak photovoltaic effect was observed for the C_{60}–OPV dyad. For the molecule having a terminal OH group, frustration of the hexagonal packing was observed and gave rise to a rare phase sequence. For this material, a columnar phase with trigonal symmetry and doubling of the crystallographic lattice was found below the hexagonal columnar phase.

Introduction

The design of functional materials for the development of the nanotechnology by the bottom-up approach has attracted growing interest in the scientific community. Liquid crystals are important materials in this area as their properties can be tuned and controlled at the molecular level up to a high degree of sophistication. As a consequence, liquid crystals have made possible the development of devices with tailor-made properties. Obviously, a detailed understanding of the characteristics and performances of the devices requires that the supramolecular organization of the liquid-crystalline components be known. For complex molecules, the *molecular structure–supramolecular organization* relationship is often difficult to establish.

Molecular shape is one of the key factors which determines the type and structure of liquid-crystalline phases: rod-like mesogens preferably form lamellar phases, whereas disc-like molecules have the tendency to form columnar phases. The hexagonal columnar phase, the most common columnar phase, is also found for molecules that do not have a well-defined disc-like shape, such as polycatenars[1] and dendrimers.[2] To generate more complex columnar phases, self-segregation at the sub-molecular level has to be considered. In this context, strong activity is devoted to the synthesis and study of hybrid materials which carry geometrically[3] and/or chemically[4] incompatible units and which are able to display unusual organizations such as laminated smectics,[5] lamello-columnar phases,[6] kagome columnar phases,[7] trigonal columnar structures[8] or hexagonal superlattices.[9] Unusual phase sequences can also be obtained.[10]

The fluidity of the mesophases makes them sensitive to external stimuli and allows the construction of mechanically/electrically/magnetically tuneable systems showing electron transport, fluorescence and lasing.[11] For example, there are attempts to design liquid crystals for application in photovoltaics by introducing strong electron donors and electron acceptors within a single mesogenic molecule in order to benefit from spontaneous nano-segregation which leads to large heterojunction surfaces.[12]

[60]Fullerene (C_{60}) is an effective electron acceptor unit and was successfully used for photovoltaic applications as an n-type semiconductor in combination with p-type π-conjugated polymers or oligomers.[13] The performances of this type of devices depend on the morphology of the film because of the phase separation which could lead to ineffective charge mobility. Interestingly, for fullerene-containing thermotropic liquid crystals,[14–21] electron transport within layered mesophases has been observed.[21] This result indicates that C_{60} can be an effective component in photovoltaics based on liquid crystal technology. However, higher charge mobility can be expected within columnar phases.[22] Thus, the design of fullerene-containing liquid crystals, which show columnar mesomorphism, in which C_{60} is covalently linked to an electron donor unit is a conceptual challenge in synthetic chemistry. Indeed, to the best of our knowledge, such materials have not yet been reported.

Functionalization of C_{60} with liquid-crystalline dendritic addends allowed the control of the mesomorphic properties as the bulky, hard C_{60} core is hidden in the dendritic matrix.[14] On the other hand, liquid-crystalline poly(benzyl ether) dendrons[23] are ideal mesomorphic promoters for the design of C_{60} derivatives which display columnar mesomorphism.[24]

We describe, herein, the synthesis, liquid-crystalline properties and supramolecular organization of a family of materials

[a]*Institut de Chimie, Université de Neuchâtel, Avenue de Bellevaux 51, 2000 Neuchâtel, Switzerland. E-mail: robert.deschenaux@unine.ch*
[b]*Department of Chemistry, University of Warsaw, ul. Zwirki i Wigury 101, 02-089 Warsaw, Poland. E-mail: pociu@chem.uw.edu.pl*
† Electronic supplementary information (ESI) available: Synthesis details, spectral characterization of compounds, example DSC trace and optical textures of observed phases. See DOI: 10.1039/c1sm05044c

built-up from three units, that are, a rod-like oligophenylenevinylene (OPV) derivative (electron donor unit), a third-generation liquid-crystalline poly(benzyl ether) dendrons (acting as columnar mesomorphism promoters) and C_{60} (electron acceptor unit) (see compounds **1–4** in Scheme 2). Preliminary photovoltaic results of C_{60}–OPV dyad **4** are also presented.

Results and discussion

Synthesis

The synthesis of **1–4** required the preparation of the OPV derivative **5** (Scheme 1). Reduction of compound **6**[25] gave bis-alcohol **7** which was reacted with carboxylic acid derivative **8** to give alcohol **9**. Esterification of the latter with benzoic acid derivative **10**[26] provided monoprotected OPV **5**. The assembly of the basic building blocks is shown in Scheme 2. Condensation of **5** with monoacid **11**[24c] (see structure in the ESI†) gave protected intermediate **1**. Deprotection of the latter with $Zn(BF_4)_2$ led to phenol derivative **2** which was reacted with third-generation poly(benzyl ether) dendron **12**[27] (see structure in the ESI†) to give malonate-based dendrimer **3**. Finally, addition of **3** with C_{60} under Bingel reaction conditions[28] gave C_{60}–OPV dyad **4**. The structure and purity of all compounds were confirmed by NMR spectroscopy, GPC (all compounds were found to be monodisperse) and elemental analysis. The presence of C_{60} in **4** was further confirmed by UV-vis spectroscopy from the observation of characteristic absorption peaks.[29]

Liquid-crystalline properties and X-ray structural studies

The liquid-crystalline properties and X-ray (XRD) data of compounds **1–4** are reported in Table 1.

No crystallization or glass transition was detected when the samples were supercooled below room temperature. They all show hexagonal columnar phases (Col_h) of *p6mm* symmetry (Fig. 1) with similar lattice parameters: $a \sim 45$ to 47 Å (Table 1).

The lattice size is only weakly temperature dependent with a negative thermal expansion coefficient lower than 0.1 Å K^{-1}. There is no difference in lattice parameters for compounds having one or two dendrons in their structure. In both cases, the column diameter corresponds roughly to the size of the disc-like molecular fragment. Apparently, for compounds **1–4**, the columnar cross-section is made of a single dendritic unit while the rod-like building blocks are randomly distributed between the columns (Fig. 1c). In the case of compounds **3** and **4** which have two dendrons per molecule, the unit cell contains half of the molecule, and the structure can be considered as intercalated columnar. Such intercalation is characteristic for molecules bearing more than one discotic unit.[30]

To further study the supramolecular organization, polarized IR experiments were performed on samples which were aligned by shearing. The anisotropy of the phenyl stretching signal (D, defined as the ratio of signal intensity for light polarized along and perpendicular to the column axis) is rather weak, *i.e.* $D \approx 0.6$, despite a nearly perfect alignment of the samples (Fig. 2). This result suggests that the molecules have a high degree of internal molecular motion. The columns should be pictured as regions where the dendritic parts of the molecules are collected rather than a stacking of flat objects, and the whole structure as a result of nano-segregation of incompatible molecular fragments. Even a lower anisotropy, *i.e.* $D \approx 1.1$, was obtained for the signals related to CH_2 symmetric and asymmetric stretching modes, showing molten state of terminal alkyl chains.

While compounds **1**, **3** and **4** display only one mesophase, compound **2**, bearing an OH group, shows a richer mesomorphism. Indeed, on cooling the sample from the highest-temperature Col_h phase, the latter transforms into another columnar phase with doubled lattice parameter (Col_{hDb}, Db stands for doubled). However, there is no noticeable

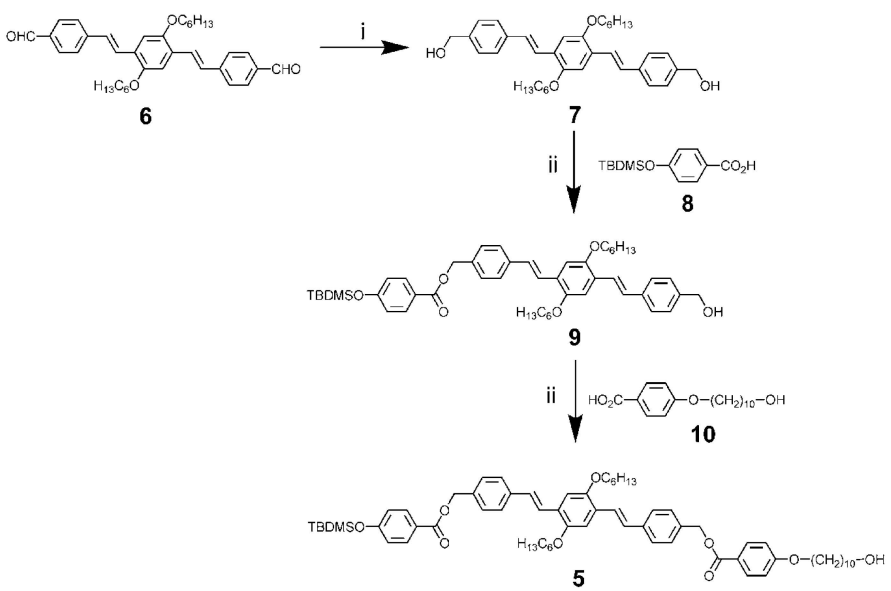

Scheme 1 (i) $LiAlH_4$, THF, rt, 2 h, 76%; (ii) *N*-(3-dimethylaminopropyl)-*N'*-ethylcarbodiimide (EDC), 4-(dimethylamino)pyridinium *p*-toluenesulfonate (DPTS), CH_2Cl_2, 0 °C and then rt, overnight; yield: for **9**, 40%; for **5**, 55%.

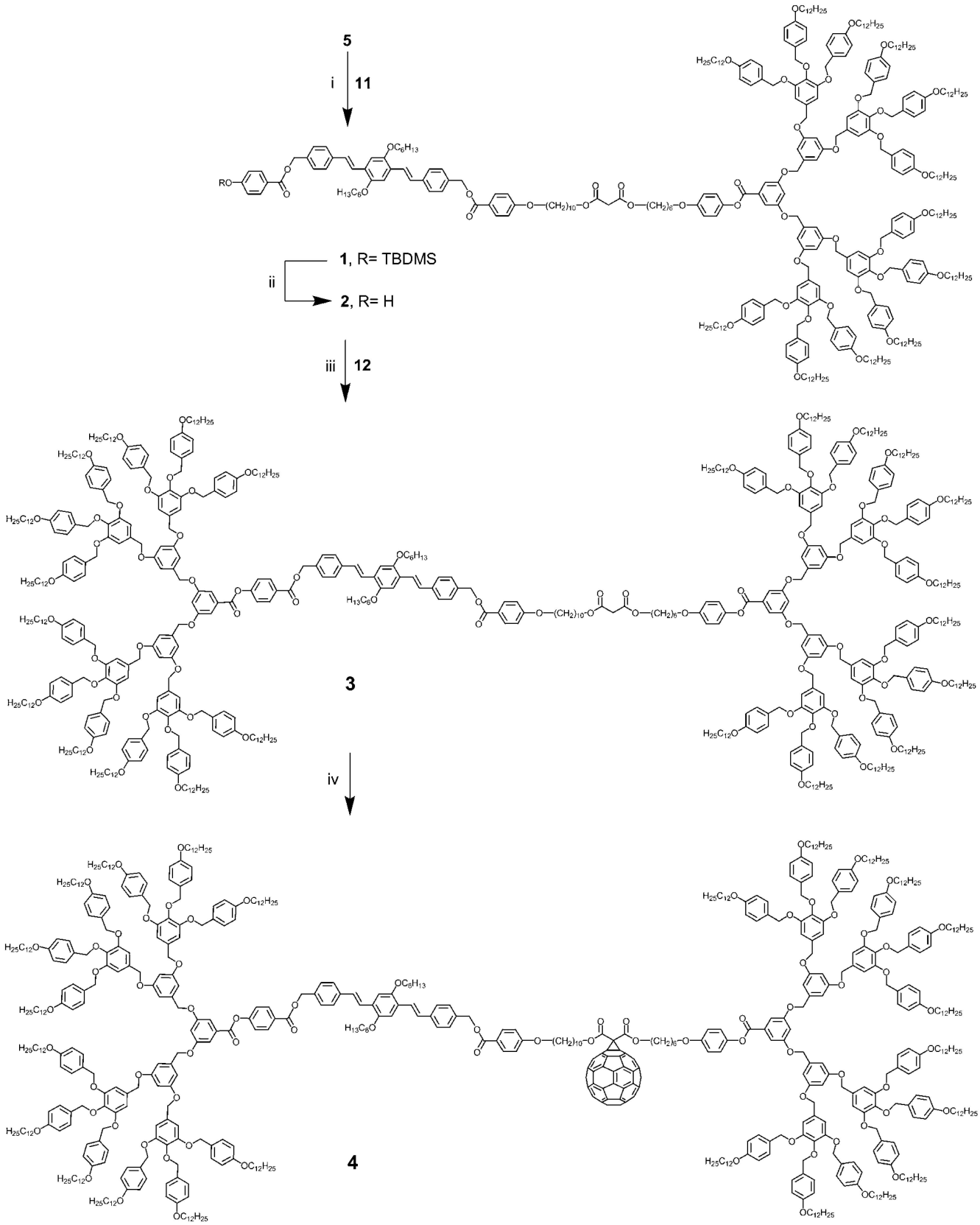

Scheme 2 (i) *N*,*N*′-Dicyclohexylcarbodiimide (DCC), 4-(dimethylamino)pyridinium *p*-toluenesulfonate (DPTS), CH_2Cl_2, 0 °C and then rt, overnight, 96%; (ii) $Zn(BF_4)_2 \cdot 6–7H_2O$, THF/H_2O, 50 °C, 24 h, 73%; (iii) DCC, DPTS, CH_2Cl_2, 0 °C and then rt, overnight, 92%; (iv) 1,8-diazabicyclo[5.4.0]undec-7-ene (DBU), I_2, toluene, rt, overnight, 69%.

Table 1 Phase-transition temperatures (in °C, heating runs), enthalpy changes (between parentheses in kJ mol^{-1}) and X-ray data

	Phase sequence	Unit cell
1	Col_h 69 (8.3) I	$a = 46.8$ Å at 50 °C
2	Col_{rDb} 48[a] Col_{hDb} 66[a] Col_h 80 (10.1) I	Col_h, $a = 46.0$ Å at 70 °C; Col_{hDb}, $a = 94.7$ Å at 50 °C; Col_{rDb}, $a = 99.4$ Å, $b = 164.5$ Å at 30 °C
3	Col_h 104 (21.8) I	$a = 47.1$ Å at 30 °C
4	Col_h 94 (19.4) I	$a = 45.8$ Å at 70 °C

[a] From X-ray studies (not detected by DSC).

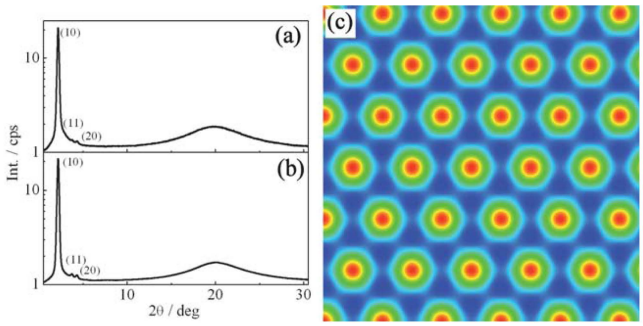

Fig. 1 X-Ray diffraction pattern for compounds **1** (a) and **3** (b) having one or two dendron units per molecule; the signals coming from hexagonal lattices for both materials are nearly at the same position. The corresponding lattice parameter is 46.8 Å and 47.1 Å for **1** and **3**, respectively. (c) Electron density map for compound **3** in the Col_h phase reconstructed form X-ray data by reverse Fourier transform taking positive square root of signal intensity as structure factor; the regions of higher electron density (columns) are made of dendrons, the regions of lower electron density are filled by rod-like fragments and aliphatic terminal chains. The size of the map is 25 × 25 nm^2.

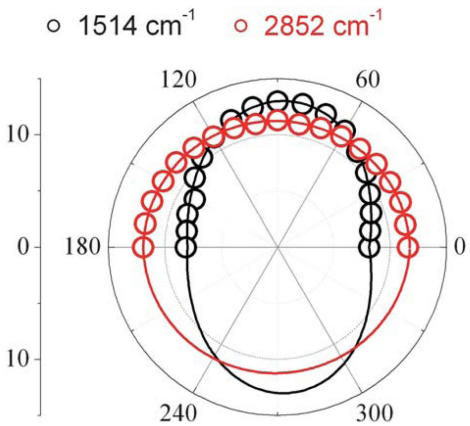

Fig. 2 Absorption of polarized IR light (arbitrary units) for aligned sample of compound **1**. Observed absorption bands at 1514 cm^{-1} and 2852 cm^{-1} are due to phenyl stretching and CH_2 symmetric stretching modes, respectively. Lines are guides for eye.

modification of the texture at the Col_h–Col_{hDb} phase transition (Polarized Optical Microscopy) nor measurable enthalpy change ($\Delta H < 0.01$ J g^{-1}). Doubling of the crystallographic unit cell is signified by the appearance of a few additional signals in the X-ray pattern (Fig. 3). In the Col_{hDb} phase, the most intense signal [indexed as (20)] remains at the same position as the (10) signal of the Col_h phase. The intensity of the (10) signal of the Col_{hDb} supperlattice is below 10% of the main (20) signal intensity, evidencing that doubling of the crystallographic lattice parameter is caused by additional, weak electron density modulation superimposed on the basic hexagonal structure. Possibly, as the temperature decreases, the rod-like molecular fragments become long-range positionally ordered in the lattice. The phase transition occurs by a stepwise increase of their correlation length. In the Col_h phase, some short range order of rod-like units is already present (correlation length ~100 Å is comparable to the lattice parameter) as indicated by the weak diffused lowest-angle signal in the X-ray pattern (Fig. 3b). In the postulated structure of the Col_{hDb} phase, the rod-like units of three neighbouring molecules are collected together. However, this requires that every fourth molecule is frustrated and the

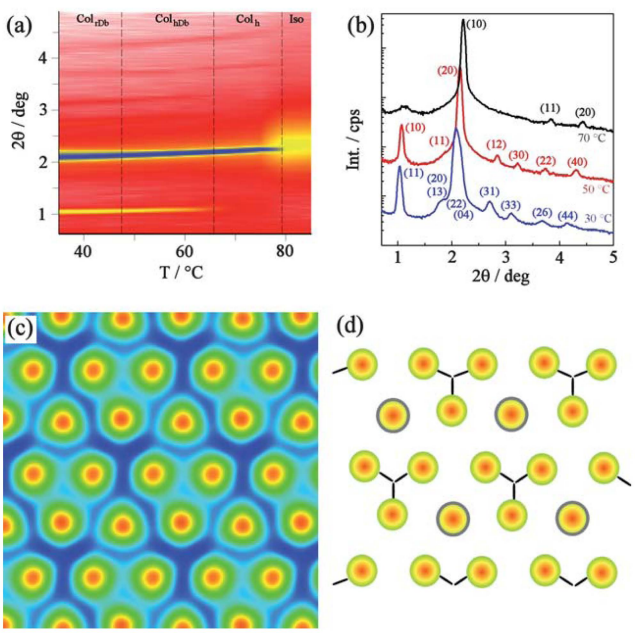

Fig. 3 (a) Temperature evolution of the positions of the X-ray signals for compound **2**; the dotted lines show phase-transition temperatures. (b) X-Ray diffraction patterns for compound **2** in the Col_h phase (70 °C, top), Col_{hDb} phase (50 °C, middle) and Col_{rDb} phase (30 °C, bottom); note that for indexing in the Col_{rDb} phase, a centred unit cell was assumed. (c) Electron density map for compound **2** in the Col_{hDb} phase; the regions of higher electron density (columns) are made of dendrons, rod-like units of three neighbouring molecules are collected together, while for every fourth molecule the position of its rod-like unit randomizes around disc. The size of the map is 25 × 25 nm^2. (d) Model of the Col_{hDb} phase structure made from disc–rod hybrid molecules; gray circles mark the molecules with randomized position of rod-like unit.

position of its rod-like unit is randomized around discs (Fig. 3d). The electron density map, reconstructed from the X-ray data (Fig. 3c), is consistent with the postulated molecular packing. In order to obtain the electron density distribution, reverse Fourier transform of the X-ray pattern was performed, taking the square root of signal intensities as structure factor amplitudes. Unfortunately, for soft matter there is no unambiguous algorithm to find structure factor phases due to a limited number of signals in the X-ray patterns. In the reverse Fourier transformation performed here, the phases of structure factors related to signals coming from the basic hexagonal lattice were taken as 0 (as in the case of the map for Col_h phase shown in Fig. 1c), while the phases of structure factors related to additional signals coming from the superlattice were taken as $\pm\pi/2$. This choice allowed the differentiation of electron density in regions between columns. Among several simulated electron density distributions the one matching the proposed structure model was chosen, the other maps had non-realistic electron density that do not agree with the molecular structures. It should be noticed that although the structure of the Col_{hDb} phase has trigonal $p3m1$ symmetry, its X-ray pattern shows $p6mm$ symmetry, as the non-resonant X-ray diffraction cannot distinguish between trigonal and hexagonal symmetries. On further cooling the sample, the hexagonal lattice of the Col_{hDb} phase deforms continuously into a rectangular one (Col_{rDb}), in which the double lattice periodicity is preserved. Distortion from the hexagonal structure measured as ratio of unit cell parameters is small: $b/a = 1.66$ was found in the Col_{rDb} phase, while for the hexagonal lattice, $b/a = \sqrt{3}$ is expected. It should be mentioned that all liquid-crystalline phases observed for compound **2** are fluid with liquid-like order inside the columns. Due to steric reasons, the molecules freeze their rotation, preserving short range positional order along the columns.

Compound **2** behaves differently than the other materials, most likely, because of hydrogen bonds between the OH groups which help to collect rod-like fragments in the inter-columnar space and allow for their long-range 2D order. The molecules terminated with the silane group, *i.e.* **1**, or a second dendron, *i.e.* **3** and **4**, have more freedom to distribute their rod-like units randomly around the columns. Thus, no long-range structure of rods is formed in the hexagonal lattice made of columns.

Photovoltaic studies

Square wave voltammetry performed for dyad **4** in TBAHFP/THF solution shows that the electrochemical gap, that is, the energy difference between the first reduction step of C_{60} and the oxidation of OPV unit, is comparable to the energy of photon of visible light (Fig. 4). The relatively small electrochemical gap (1.7 eV) gives a strong hint that the photoexcited state of compound **4** might relax by a non-radiative mechanism to the charge separated state with electrons on C_{60} and holes on OPV. Indeed, large decrease of fluorescence intensity (by a factor of 7) and shortening of fluorescence life-time were observed for compound **4** in comparison to the C_{60}-free precursor **3** (Fig. 5).

The formation of a charge-separated state was confirmed by a small but clear photovoltaic effect in the liquid-crystalline state (Fig. 4). In the experiment, the sample was deposited onto an ITO electrode as a thin film and covered with conductive solution; the system was exposed to increasing voltage and periodically illuminated. The low value of photocurrent might be explained by poor space separation of the OPV and C_{60} units, causing fast charge recombination.

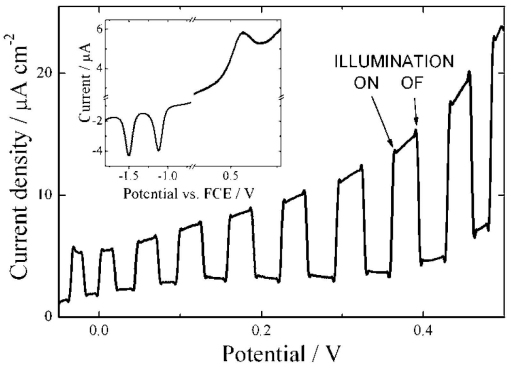

Fig. 4 Photocurrent observed for compound **4**; inset: square wave voltammogram for compound **4** recorded in 0.1 M TBAHFP/THF showing the first two reduction steps of C_{60} (at −1.119 V and −1.501 V) and the oxidation of OPV (at 0.566 V).

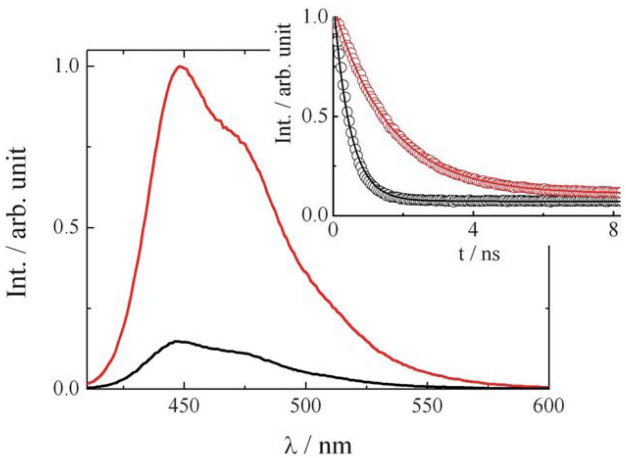

Fig. 5 Emission spectra (excitation at 390 nm) for compounds **3** (red) and **4** (black) in CH_2Cl_2 (both solutions at the same concentration); inset: fluorescence intensity (at 450 nm, excitation at 335 nm) *vs.* time. Lines are fits to exponential decay with single relaxation time, being 1.59 ns and 0.47 ns for **3** and **4**, respectively.

Conclusions

We have shown that rod–disc hybrid mesogens easily form columnar phases, even if they contain a bulky C_{60} cage in the molecular structure. Competition between steric interactions and hydrogen bonding might cause frustration in hexagonal lattice. In order to reduce the frustration, the system develops additional order of rods superimposed on the hexagonal columnar structure of discs. Fullerene derivative **4** shows photovoltaic effect in the columnar phase. The effect is small since there are not well-defined 'channels' in the structure transporting electrons and holes.

Acknowledgements

The work was supported by MNISW grant 'Iuventus Plus' (IP2010-036570) and the Swiss National Science Foundation (Grant No 200020-119648).

References

1 E. Gorecka, D. Pociecha, J. Mieczkowski, J. Matraszek, D. Guillon and B. Donnio, *J. Am. Chem. Soc.*, 2004, **126**, 15946.

2 (*a*) B. Donnio and G. Guillon, *Adv. Polym. Sci.*, 2006, **201**, 45; (*b*) B. Donnio, S. Buathong, I. Bury and D. Guillon, *Chem. Soc. Rev.*, 2007, **36**, 1495.

3 (*a*) J. J. Hunt, R. W. Date, B. A. Timimi, G. R. Luckhurst and D. W. Bruce, *J. Am. Chem. Soc.*, 2001, **123**, 10115; (*b*) P. H. J. Kouwer and G. H. Mehl, *Angew. Chem., Int. Ed.*, 2003, **42**, 6015; (*c*) P. H. J. Kouwer and G. H. Mehl, *J. Am. Chem. Soc.*, 2003, **125**, 11172.

4 (*a*) B. Chen, U. Baumeister, S. Diele, M. Kumar Das, X. Zeng, G. Ungar and C. Tschierske, *J. Am. Chem. Soc.*, 2004, **126**, 8608; (*b*) F. Liu, B. Chen, U. Baumeister, X. Zeng, G. Ungar and C. Tschierske, *J. Am. Chem. Soc.*, 2007, **129**, 9578; (*c*) M. Prehm, F. Liu, X. Zeng, G. Ungar and C. Tschierske, *J. Am. Chem. Soc.*, 2008, **130**, 14922.

5 X. Hong Cheng, M. Kumar Das, S. Diele and C. Tschierske, *Angew. Chem., Int. Ed.*, 2002, **41**, 4031.

6 (*a*) J. Malthête, A.-M. Levelut and L. Liebert, *Adv. Mater.*, 1992, **4**, 37; (*b*) L. Cui, J. Miao and L. Zhu, *Macromolecules*, 2006, **39**, 2536; (*c*) L. Cui and L. Zhu, *Langmuir*, 2006, **22**, 5982.

7 B. Glettner, F. Liu, X. Zeng, M. Prehm, U. Baumeister, M. Walker, M. A. Bates, P. Boesecke, G. Ungar and C. Tschierske, *Angew. Chem., Int. Ed.*, 2008, **47**, 9063.

8 B. Glettner, F. Liu, X. Zeng, M. Prehm, U. Baumeister, G. Ungar and C. Tschierske, *Angew. Chem., Int. Ed.*, 2008, **47**, 6080.

9 V. Percec, C.-H. Ahn, T. K. Bera, G. Ungar and D. J. P. Yeardley, *Chem.–Eur. J.*, 1999, **5**, 1070.

10 A. Glebowska, P. Przybylski, M. Winek, P. Krzyczkowska, A. Krówczynski, J. Szydlowska, D. Pociecha and E. Górecka, *J. Mater. Chem.*, 2009, **19**, 1395.

11 P. Palffy-Muhoray, W. Cao, M. Moreira, B. Taheri and A. Munoz, *Philos. Trans. R. Soc., A*, 2006, **364**, 2747.

12 M. Carrasco-Orozco, W. C. Tsoi, M. O'Neill, M. P. Aldred, P. Vlachos and S. M. Kelly, *Adv. Mater.*, 2006, **18**, 1754.

13 (*a*) G. Yu, J. Gao, J. C. Hummelen, F. Wudl and A. J. Heeger, *Science*, 1995, **270**, 1789; (*b*) J.-F. Nierengarten, J.-F. Eckert, J.-F. Nicoud, L. Ouali, V. Krasnikov and G. Hadziioannou, *Chem. Commun.*, 1999, 617; (*c*) J.-F. Eckert, J.-F. Nicoud, J.-F. Nierengarten, S.-G. Liu, L. Echegoyen, F. Barigelletti, N. Armaroli, L. Ouali, V. Krasnikov and G. Hadziioannou, *J. Am. Chem. Soc.*, 2000, **122**, 7467; (*d*) H. Hoppe, D. A. M. Egbe, D. Mühlbacher and N. S. Sariciftci, *J. Mater. Chem.*, 2004, **14**, 3462; (*e*) W. Ma, C. Yang, X. Gong, K. Lee and A. J. Heeger, *Adv. Funct. Mater.*, 2005, **15**, 1617; (*f*) J. L. Segura, N. Martín and D. M. Guldi, *Chem. Soc. Rev.*, 2005, **34**, 31; (*g*) H. Hoppe and N. S. Sariciftci, *J. Mater. Chem.*, 2006, **16**, 45; (*h*) J. Y. Kim, K. Lee, N. E. Coates, D. Moses, T.-Q. Nguyen, M. Dante and A. J. Heeger, *Science*, 2007, **317**, 222.

14 (*a*) R. Deschenaux, B. Donnio and D. Guillon, *New J. Chem.*, 2007, **31**, 1064; (*b*) S. Campidelli, P. Bourgun, B. Guintchin, J. Furrer, H. Stoeckli-Evans, I. M. Saez, J. W. Goodby and R. Deschenaux, *J. Am. Chem. Soc.*, 2010, **132**, 3574; (*c*) F. Lincker, P. Bourgun, H. Stoeckli-Evans, I. M. Saez, J. W. Goodby and R. Deschenaux, *Chem. Commun.*, 2010, **46**, 7522.

15 D. Felder, B. Heinrich, D. Guillon, J.-F. Nicoud and J.-F. Nierengarten, *Chem.–Eur. J.*, 2000, **6**, 3501.

16 N. Tirelli, F. Cardullo, T. Habicher, U. W. Suter and F. Diederich, *J. Chem. Soc., Perkin Trans. 2*, 2000, 193.

17 (*a*) M. Sawamura, K. Kawai, Y. Matsuo, K. Kanie, T. Kato and E. Nakamura, *Nature*, 2002, **419**, 702; (*b*) C.-Z. Li, Y. Matsuo and E. Nakamura, *J. Am. Chem. Soc.*, 2009, **131**, 17058.

18 R. J. Bushby, I. W. Hamley, Q. Liu, O. R. Lozman and J. E. Lydon, *J. Mater. Chem.*, 2005, **15**, 4429.

19 (*a*) D. Felder-Flesch, L. Rupnicki, C. Bourgogne, B. Donnio and D. Guillon, *J. Mater. Chem.*, 2006, **16**, 304; (*b*) H. Mamlouk, B. Heinrich, C. Bourgogne, B. Donnio, D. Guillon and D. Felder-Flesch, *J. Mater. Chem.*, 2007, **17**, 2199.

20 A. de la Escosura, M. V. Martínez-Díaz, J. Barberá and T. Torres, *J. Org. Chem.*, 2008, **73**, 1475.

21 (*a*) T. Nakanishi, Y. Shen, J. Wang, S. Yagai, M. Funahashi, T. Kato, P. Fernandes, H. Möhwald and D. G. Kurth, *J. Am. Chem. Soc.*, 2008, **130**, 9236; (*b*) W.-S. Li, Y. Yamamoto, T. Fukushima, A. Saeki, S. Seki, S. Tagawa, H. Masunaga, S. Sasaki, M. Takata and T. Aida, *J. Am. Chem. Soc.*, 2008, **130**, 8886.

22 S. Laschat, A. Baro, N. Steinke, F. Giesselmann, C. Hägele, G. Scalia, R. Judele, E. Kapatsina, S. Sauer, A. Schreivogel and M. Tosoni, *Angew. Chem., Int. Ed.*, 2007, **46**, 4832.

23 B. M. Rosen, C. J. Wilson, D. A. Wilson, M. Peterca, M. R. Imam and V. Percec, *Chem. Rev.*, 2009, **109**, 6275.

24 (*a*) J. Lenoble, N. Maringa, S. Campidelli, B. Donnio, D. Guillon and R. Deschenaux, *Org. Lett.*, 2006, **8**, 1851; (*b*) J. Lenoble, S. Campidelli, N. Maringa, B. Donnio, D. Guillon, N. Yevlampieva and R. Deschenaux, *J. Am. Chem. Soc.*, 2007, **129**, 9941; (*c*) N. Maringa, J. Lenoble, B. Donnio, D. Guillon and R. Deschenaux, *J. Mater. Chem.*, 2008, **18**, 1524.

25 G. de la Torre, F. Giacalone, J. L. Segura, N. Martín and D. M. Guldi, *Chem.–Eur. J.*, 2005, **11**, 1267.

26 B. Dardel, D. Guillon, B. Heinrich and R. Deschenaux, *J. Mater. Chem.*, 2001, **11**, 2814.

27 V. Percec, W.-D. Cho, G. Ungar and D. J. P. Yeardley, *J. Am. Chem. Soc.*, 2001, **123**, 1302.

28 C. Bingel, *Chem. Ber.*, 1993, **126**, 1957.

29 (*a*) D. M. Guldi, *Chem. Commun.*, 2000, 321; (*b*) D. M. Guldi, *Chem. Soc. Rev.*, 2002, **31**, 22.

30 A. Zelcer, B. Donnio, C. Bourgogne, F. D. Cukiernik and D. Guillon, *Chem. Mater.*, 2007, **19**, 1992.